Proceedings of the XVII ECSMGE-2019
Geotechnical Engineering foundation of the future
ISBN 978-9935-9436-1-3

doi: 10.32075/17ECSMGE-2019-0415

XVII European Conference
ECSMGE 2019
Reykjavík
on Soil Mechanics
and Geotechnical Engineering

Performance and modelling of a deep excavation in the context of the Grand Paris project

Performance et modélisation d'une excavation profonde dans le contexte du projet du Grand Paris

K. Nejjar[1], A. Boffa[2], D. Dias[3], F. Cuira[1], P. Vidil[2], H. Le Bissonnais[1], G. Chapron[1]
[1]*Terrasol, Paris, France*

[2]*Soletanche-bachy, Paris, France*

[3]*3SR Laboratory Grenoble Alpes University, Grenoble, France*

ABSTRACT: As part of the Grand Paris project, several stations of the new subway line 15 will be excavated to significant depths up to 40 m in urban sites and supported by braced retaining walls. The latter face not only exceptional geometry but also the particular Parisian geology with an overconsolidated plastic clay. The classical subgrade reaction method used to design the retaining wall does not take into account the arching effect that may occur between support elements; whereas finite element modelling affords the development of this effect and allows to highlight load transfers. In situations where the pore water pressure is low, it may lead to significant differences in terms of loads in struts between those two methods.
For the design of the new station in construction Fort d'Issy Vanves Clamart, a comparative study was carried out between finite element modelling and the subgrade reaction method. Convergent results were found in terms of wall displacement and bending moment, provided accurate choice of inputs. However, great differences were noticed for loads in support elements. The results are compared with the real performance of the retaining wall. Wall displacement and strut loads measurements are presented in addition to advanced instrumentation with pressure cells and fiber optic.

RÉSUMÉ: Dans le contexte du projet du Grand Paris, plusieurs gares de la nouvelle ligne 15 sont excavées à des profondeurs importantes jusqu'à 40m et à l'abri de parois moulées butonnées. Ces dernières doivent non seulement soutenir une fouille de géométrie exceptionnelle mais aussi une géologie atypique avec la présence de la couche d'Argile Plastique surconsolidée. La méthode des coefficients de réaction classiquement utilisée pour la conception de ces ouvrages ne prend pas en compte l'effet de voûte qui se produit entre les éléments d'appuis rigides; tandis que les modélisations numériques à bases d'éléments finis permettent le transfert de charge par cisaillement dans le sol et ainsi le développement des arcs de voûte. Lorsque les pressions hydrostatiques sont faibles, ces deux méthodes peuvent conduire à des écarts significatifs d'efforts dans les butons.
Le présent article présente une étude comparative entre ces deux méthodes appliquées sur le cas de la nouvelle gare en cours de construction Fort d'Issy Vanves Clamart. Malgré la convergence des résultats en termes de déformée de l'écran et de moment, les efforts dans les appuis mettent en évidence une différence claire entre les deux méthodes. Ces résultats ont été comparés avec le comportement réel de la paroi à travers les mesures de l'instrumentation mise en place à savoir des tubes inclinométriques, des jauges de déformations, de la fibre optique et des cellules de pression.

Keywords: Deep excavation; subgrade reaction method; finite element method; arching effect

1 INTRODUCTION

Modelling braced excavations with the subgrade reaction method (SRM) is a common practice in France. The relevance of that method is recognized by dozens of years of practice and geotechnical monitoring; its simplicity and immediate computation time make its use appropriate for worksite execution report. However, Vezole (1995) has questioned the SRM pointing out the inaccuracy of considering proportionality between pressure and displacement for each wall element independently of adjacent elements. The great development of finite element method (FEM) affords advanced tools to model correctly the soil structure interaction, taking into account the soil behavior behind the wall as a continuum medium involving the whole stress tensor. FEM was widely used to model historical deep excavations in order to assess ground settlements behind the wall especially when sensitive buildings are exposed nearby (Kung 2009, Dong 2014, Schwamb 2015). However, FEM is often time-consuming and requires vigilant user to supply such complex models with appropriate input parameters.

The Grand Paris project offers an excellent opportunity to explore the limits of SRM facing up to the real performance of several deep excavations up to 40m. The purpose is to understand the physical phenomenon responsible of observed discrepancies between SRM and FEM outputs and assess their impact on the design in order to guide the engineer judgment to know the limit of each method depending on the requirement of the project.

2 THE SITE

Fort-d'Issy-Vanves-Clamart is the first metro station under construction of the new subway line 15 of the Grand Paris project. It is a rectangular shaped station of 110 m long by 23m large and 32 m deep. The excavation is supported by 1.2 m thick retaining wall and several levels of struts and floor slabs. The present article presents the performance of the wall only up to 20 m deep regarding work progress.

The analyzed section is shown in the Figure 1 with the monitoring system used. The latter is composed of two inclinometers (N=north, S=south), 3 strain gauges in each monitored strut in both levels B1 and B2, 100 m of fiber optic installed in one wall panel and a pressure cell at the interface soil/wall in the excavation side at a depth of 34.5 m.

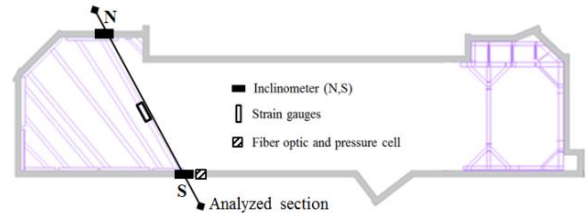

Figure 1: Top view of the station and instrumentation location

Figure 2 presents the excavation geometry, the support elements and soil stratigraphy with the horizontal soil layer classical of the Parisian sedimentary basin. The section considered follows the struts, however, only the south wall is concerned by the slabs.

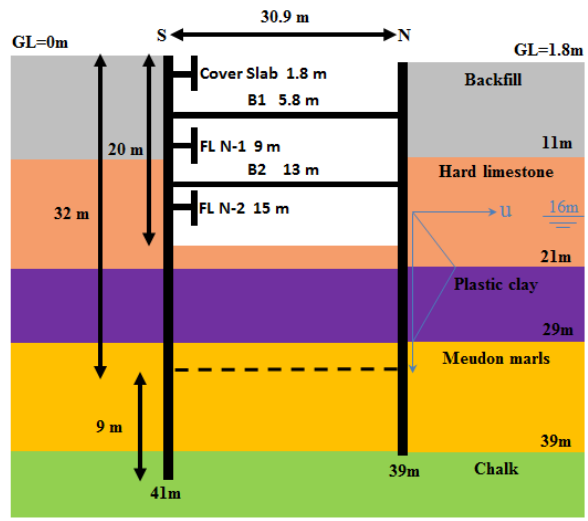

Figure 2: Cross sectional view of the soil stratigraphy

The stratigraphy is composed of a backfill of 11 m height, 10 m of damaged Hard limestones, 8 m of Plastic clays, 10 m of Meudon marls and Chalk. The groundwater table is located at 16 m deep in the Hard limestones. The steady state profile of water pressure is drawn in blue in Figure 2. The pressure is supposed decreasing linearly to zero in Plastic clay layer due to its low permeability. It has to be noted that the water has very little influence on the design of this station.

Table 1 presents the geotechnical properties issued from in situ and laboratory soil tests namely the dynamic shear modulus G_0 from cross hole seismic test, the pressuremeter modulus E_M and its rheological coefficient α depending on soil type (Ménard 1968), the shear strength parameters respectively friction angle φ' and cohesion c', the overconsolidation ratio OCR and the earth pressure coefficient at rest K_0 deduced from Mayne and Kulhawy (1982) correlation.

Table 1: Geotechnical properties of soil layers

	Backfill	Hard Limestone	Plastic Clay	Meudon Marls	Chalk
G_0 (MPa)	175	600	156	670	950
E_M (MPa)	6	25	40	100	170
α	0.5	0.5	1	0.67	0.5
φ' (°)	29	35	18	25	35
c' (kPa)	0	40	10	30	40
OCR	1	1	1.5	1	1
K_0	0.52	0.43	0.85	0.58	0.43

The construction phases are detailed herein:

- Initialization of the stress state taking into account a surcharge loads of 30 kPa due to nearby traffic
- Installation of north diaphragm wall at ground level GL=1.8 m
- Excavation with slope at 7.5 m deep and installation of south diaphragm wall
- Extend south wall upward to ground level GL=0 m and backfill the slope
- Set up cover slab for south wall at 1.8 m deep
- Set up strut level B1 at 5.8 m prestressed at 148 kN/lm
- Excavation at 10 m deep
- Set up N-1 floor level for south wall at 9 m
- Excavation at 14.2 m deep
- Set up strut level B2 at 13 m prestressed at 595 kN/lm
- Excavation at 16.5 m deep
- Set up N-2 floor level for south wall at 15 m
- Excavation at 20 m

Based on design report, stiffnesses of support elements for 2D modelling are summarized in the Table 2. The wall has an inertia product of EI=3456MN.m²/lm. The north wall (N) goes down to 39m deep and the south wall (S) to 41 deep (Figure 2).

Table 2: Stiffness of support elements

	Stiffness (MN/m/lm)
Cover slab	2760
Strut B1	60
Floor Level N-1	280
Strut B2	122
Floor Level N-2	160

3 FINITE ELEMENT AND SUBGRADE REACTION MODEL

Finite element modelling (FEM) was carried out with Plaxis 2D v.2017 and the subgrade reaction model (SRM) with Paris (Internal software of Soletanche Bachy).

For FEM, the advanced soil model HSS is used for all soils (Plaxis manual). HSS is a hardening soil model taking into account small-strain stiffness by including a shear modulus degradation curve following Hardin&Drnevich (1972)

sigmoïdal model that involves two parameters G_0 and $\gamma_{0.7}$ (Eq.1).

$$G = \frac{G_0}{1+0.385\frac{\gamma}{\gamma_{0.7}}} \quad (1)$$

G_0 corresponds to the dynamic shear modulus and $\gamma_{0.7}$ is the distortion reached at 70% of modulus reduction.

For normally consolidated soil, the parameter $\gamma_{0.7}$ could be assessed with Benz (2007) formula (Eq.2) where σ'_1 is the vertical stress at the middle of the layer.

$$\gamma_{0.7} = \frac{3}{28G_0}(2c'(1+\cos(2\varphi')) + \sigma'_1(1+K_0)\sin(2\varphi')) \quad (2)$$

For the overconsolidated layer of Plastic clay, the parameter $\gamma_{0.7}$ was determined to fit with the measured $(E_{50}, \gamma_{E_{50}})$ from triaxial tests.

The Table 3 summarizes inputs of HSS soil model. E_{50} is taken equal to 2.5 times the measured E_M/α. By default, E_{oed} is taken equal to E_{50} and E_{ur} is the double except for Backfill which is taken the triple.

Table 3: Inputs of HSS soil model

	Backfill	Hard limestone	Plastic clay	Meudon marls	Chalk
E_{50} (MPa)	30	125	100	375	850
E_{oed} (MPa)	30	125	100	375	850
E_{ur} (MPa)	90	250	200	750	1700
ν_{ur}	0.2	0.2	0.2	0.2	0.2
m	0	0	0	0	0
$\varphi'(°)$	29	35	18	25	35
c' (kPa)	0	40	10	30	40
K_0	0.52	0.43	0.85	0.58	0.43
R_{inter}	0.66	0.66	0.33	0.66	0.66
G_0 (MPa)	175	600	156	670	950
$\gamma_{0.7}$	9.5E-5	9.0E-5	1.0E-4	1.5E-4	1.3E-4

For SRM, the formula of Schmitt (1995) is used to compute the reaction coefficient k_h using the wall inertia and 1.5 times the measured E_M/α.

The coefficients 2.5 and 1.5 have been chosen to have the best fitting between measured displacements and numerical results.

4 WALL DISPLACEMENT AND MOMENT

Wall displacements are measured from the inclinometers placed in the north and south wall panels (N and S). The Figure 3 shows a good agreement between both FEM and SRM models and the real performance of the retaining wall in terms of general shape and maximum value. However, SRM model shows for north wall a small displacement to the soil at the top of the wall. It could be related to the fact that SRM doesn't take into account the continuous medium behind the wall in this particular case of high prestressing.

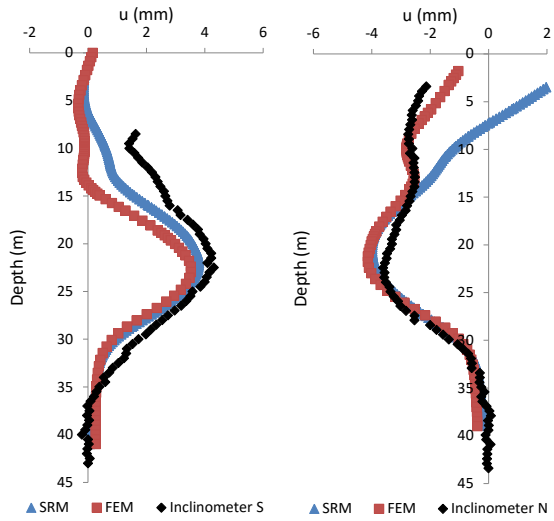

(a) (b)

Figure 3: Wall displacements compared with SRM and FEM models: (a) south wall, (b) north wall

Bending moment is measured with the fiber optic installed in the south wall. Figure 4 illustrates a good concordance between modelling and measurements in terms of moment shape and location of the maximum moment.

The performance of retaining wall to 20 m excavation deep confirms the relevance of the FEM and SRM modelling in terms of reproducing wall displacements and bending moments. Hence, SRM is largely sufficient to predict wall displacement and bending moment, the recourse to FEM models seems not necessary. For complex projects, those two methods are used simultaneously in order to adjust moduli if necessary.

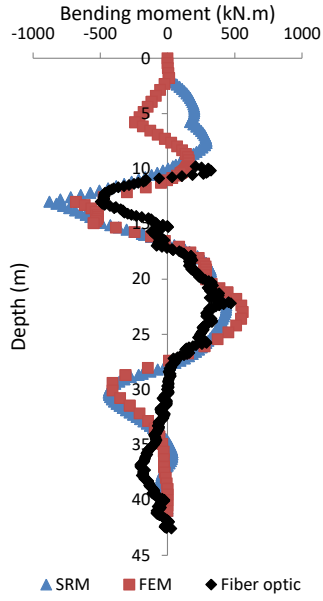

Figure 4: Bending moment of the south wall compared with SRM and FEM models

5 STRUT FORCE

In order to assess the performance of the support elements, two struts are monitored with strains gauges. 3 gauges are fixed on each cylindric strut and spaced by 120°, hence the force is computed from the mean value of the three gauges multiplied by the steel modulus of 210 GPa and the strut section (0.024m² for B1 and 0.049m² for B2). As FEM and SRM are 2D models, the measured value is converted to 2D value by taking into account the inclination angle of 30° and the spacing of struts (4.1 m). Hence the converted value could be compared to the force issued from modelling. Temperature is also measured at the same time frequency as strain gauges. It is interesting to notice that temperature is measured at the strain gauge welded on the strut, the measured temperature is therfore the strut one. Figure 5 and Figure 6 present the evolution of the strut force with the temperature during the term of modeled excavation. The blue points are measurements few days after prestress and red points are few days before the beginning of the next phase of excavation not concerned in this analysis. One can see that the strut force varies mostly linearly with temperature. We can consider that it varies by a slope corresponding to 0.8ESβ, to be compared to 1.0ESβ for infinitely rigid supports, where E is the steel modulus, S is the section and β is the dilatation coefficient of steel equal to 1.2 10^{-5}. Two lines with this slope are drawn to delimit the increment of strut force (from the prestress) due to excavation independently of temperature ΔF. This increment is the measured value to be compared to modeling.

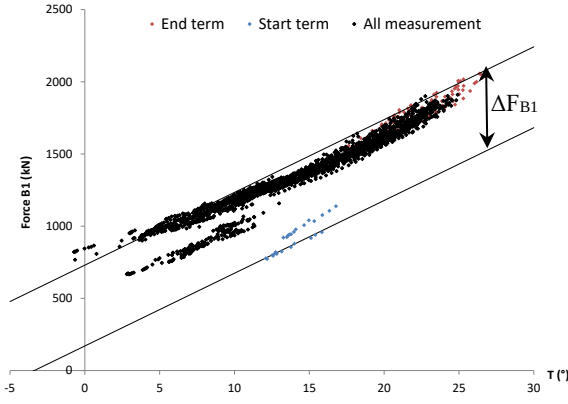

Figure 5: Strain gauges measurement and temperature on strut B1

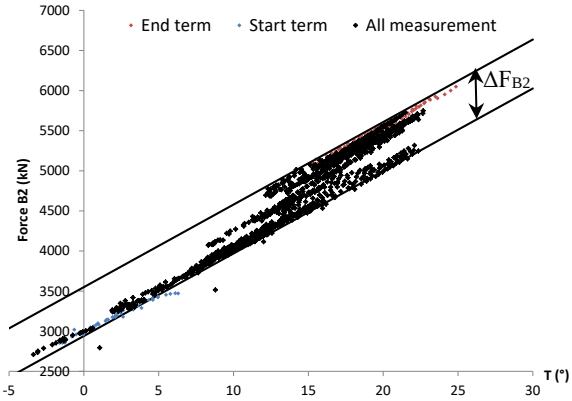

Figure 6: Strain gauges measurement and temperature on strut B2

Table 4 presents the strut forces computed from SRM and FEM. ΔF is the difference between the maximum force in all modelling phases and the prestress force.

For the strut B1, both models agree on a similar computed force of 80kN/lm. However this value is 32% lower than the measured value. For the strut B2, FEM presents a higher computed force than SRM. Since the input structure stiffness is the same in both models, this difference is due to a different computed lateral earth pressure behind the wall. Indeed, FEM models the soil as a continuum medium where shearing stresses develop and allow for load transfer to take place between soil layers. Hence rigid support elements are more loaded than the other flexible areas along the retaining wall because of stress redistribution. In contrast, SRM considers a Winkler approach with horizontal springs completely independent from one another, hence stress redistribution is dismissed and strut force may be underestimated.

The measured increment falls between the two values predicted by FEM and SRM. Indeed, FEM overestimates the increment by +35% (45 kN/lm) where SRM underestimates it by -33% (43 kN/lm).

Table 4: Comparison of the increment in strut forces between SRM, FEM and strain gauges

	ΔF_{B1} (kN/lm)	ΔF_{B2} (kN/lm)
Strain gauges	118	129
SRM	79	86
FEM	80	174

It should be recalled that the strut load is the sum of the prestressing force, the increment between the previous stage, and the load due to temperature gradient. Besides, it has to be noted that this case study deals with very high prestressing (148 kN/ml for B1 and 595 kN/ml for B2) and it should be interesting to compare those figures with another station with no prestressing at all.

6 LATERAL EARTH PRESSURE

The Figure 7 presents the pressure in front of the wall in excavation side located at 34.5m compared with the pressure cell installed at soil/wall interface at the final excavation phase. FEM predicts higher pressure than SRM which concurs with the precedent remark about the difference in computed earth pressure between the two models. The pressure cell shows a higher value than FEM by 30%. However, the cell could overestimate the measured pressure by at most +15% due to edge effect related to the presence of the cell itself at soil/wall interface (Geokon 2017). Taking account this eventual overestimation of the measure, FEM predicts a pressure slightly lower than the cell by -17% whereas SRM underestimates the pressure by -46%.

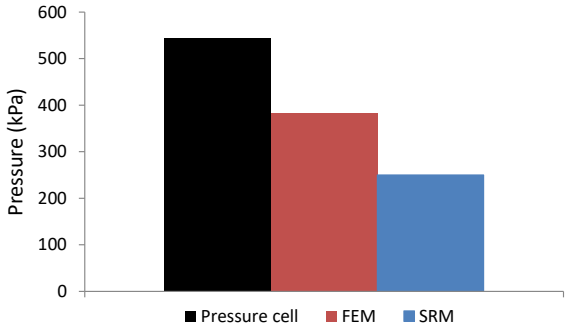

Figure 7:Earth pressure in the excavated side at 34.5m deep

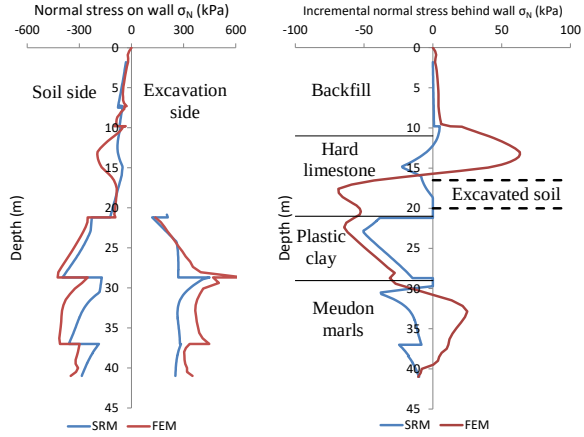

Figure 8: Earth pressure on the wall, (a) normal stress of both wall sides at final excavation phase, (b) incremental normal stress behind the wall at final excavation phase

Figure 8 (a) shows the earth pressure diagram behind and in front of the wall at the final excavation phase. FEM produces higher pressure in both sides compared to SRM. To better understand the cause of this final distribution since both models start with the same initial stress state set by K_0, Figure 8 (b) shows the variation in normal stress behind the wall during only the final excavation phase. SRM diagram predicts systematically a decreasing stress along the wall where FEM reveals a specific diagram typical for the occurrence of stress redistribution. Indeed, a great depression is produced behind the wall at the zone of excavated soil and the Plastic clay. Simultaneously, two compression zones appear at the top and the bottom of the wall where the latter is stiffened by the presence of support elements at the top and the presence of the stiffer layer of Meudon marls (yet in place) at the bottom.

The earth pressure distribution behind and in front of the wall reveals the major difference between SRM and FEM models. The latter allows the development of arching effect whereas SRM ignores this phenomenon. Since the consequences on strut force could be significant in some cases (Oslo subway Bjerrum et al. 1972), the recourse to FEM models to assess this impact may be necessary.

7 CONCLUSION

The advanced monitoring of the new metro station Fort-d'Issy-Vanves-Clamart affords to assess the retaining wall performance in terms of wall displacement, bending moment, strut forces, and mobilized earth pressure in front of the wall. It allows hence checking different output of design modelling in order to provide a complete analysis.

FEM and SRM were both used to model the excavation up to 20 m deep. Results shows that an amplification of E_M/α by 1.5 for SRM and a secant modulus E_{50} equal to $2.5E_M/\alpha$ is sufficient to reproduce the same wall displacement and bending moment as measurements for both models. However, differences emerge when

comparing strut forces and earth pressure in front of the wall. For strut, FEM seems to over-estimates the force increment by +35% where SRM underestimates them by -33%. For earth pressure in front of the wall, FEM predicts a slightly lower value than measurement by -17% whereas SRM underestimates the earth pressure by -46%. The analysis of the computed earth pressure diagram behind the wall pointed out the arching effect is the main responsible of those differences. Indeed, FEM sees the soil as a continuum medium where shear stress are allowed and transfer load mechanisms could take place to overload rigid zones of the wall namely the top and the bottom. SRM considers the soil/wall interaction as independent horizontal springs which dismiss any stress redistribution.

In conclusion, SRM seems largely sufficient to predict wall displacement and bending moment. However it could have a stress distribution different from FEM and reality, which could lead to underestimate the forces in some strut elements in particular in situations where the pore water pressure is low and to a different passive earth pressure distribution. Hence FEM may be needed to assess the impact of arching on load redistribution.

The present analysis of measurements should be corroborated by further excavation phases until the final excavation level of 32 m deep.

8 ACKNOWLEDGMENTS

The writers would like to thank the Société du Grand Paris for financial support of the installation of advanced monitoring. We would like to warmly thank our partners in this work namely Lerm, Gexpertise, Ifsttar, Geokon and Dimione. We express our gratitude for the precious support of worksite teams of both Soletanche Bachy and Bouygues TP.

9 REFERENCES

Benz T., 2007, Small-Strain Stiffness of soils and its numerical consequences, Universität Stuttgart

Bjerrum L., Frimann Clause C.J., Duncan J. M. 1972, Earth pressures on flexibles structures – a state of the art report, 5th European Conference on Soil Mechanics and Foundation Engineering, Madrid, pp. 169-193

Dong Y. 2014, Advanced finite element analysis of deep excavation case histories,

Geokon Instruction Manual 2017, Model 4800 series, VW Earth Pressure Cells

Kung G.T.C, Ou c.Y, Juang H. 2009, Modeling small-strain behavior of Taipei clays for finite element analysis of braced excavations, Computers and Geotechnics 36, pp. 304-319

Hardin B.O, Drnevich V.P 1972, Shear modulus and damping in soils: Design equations and curves. Proc. ASCE: Journal of thr Soil Mechanics and Foundations Division, 98(SM7), 667-692

Mayne P.W., Kulhawy F.H, 1982, K0-OCR relationships in soil, Journal of the Geotechnical Engineering Division, Proceedings of ASCE, Vol 108, N° GT6, pp 851-869

Ménard L. 1968, Règles d'exploitation des techniques pressiométriques et d'exploitation des résultats obtenus pour le calcul des fondations, Sols-Soils, N°26 Paris

Schmitt P. 1995, Méthode empirique d'évaluation du coefficient de reaction du sol vis à vis des ouvrages de soutènement souples, Revue française de Géotehnique, 71, pp. 3-10

Schwamb T. Soga K. 2015, Numerical modelling of a deep circular excavation Abbey Mills in London, Géotechnique 65, N° 7, pp. 604-619

Vezole P. 1995, Retaining walls Ground-Structure interaction about the reaction coefficients method, Revue Française de Géotechnique, N° 71, 2ème trimestre, pp 31-37